Transverse instability and dynamics of nonlocal bright solitons

G. N. Koutsokostas,[1] G. Theocharis,[2] T. P. Horikis,[3] P. G. Kevrekidis,[4] and D. J. Frantzeskakis[1]
[1]*Department of Physics, National and Kapodistrian University of Athens, Panepistimiopolis, Zografos, Athens 15784, Greece*
[2]*LAUM, CNRS, Le Mans Université, Avenue Olivier Messiaen, 72085 Le Mans, France*
[3]*Department of Mathematics, University of Ioannina, Ioannina 45110, Greece*
[4]*Department of Mathematics and Statistics, University of Massachusetts, Amherst, Massachusetts 01003-4515, USA*

(Received 18 May 2021; accepted 22 November 2021; published 9 December 2021)

We study the transverse instability and dynamics of bright soliton stripes in two-dimensional nonlocal nonlinear media. Using a multiscale perturbation method, we derive analytically the first-order correction to the soliton shape, which features an exponential growth in time—a signature of the transverse instability. The soliton's characteristic timescale associated with its exponential growth is found to depend on the square root of the nonlocality parameter. This, in turn, highlights the nonlocality-induced suppression of the transverse instability. Our analytical predictions are corroborated by direct numerical simulations, with the analytical results being in good agreement with the numerical ones.

DOI: 10.1103/PhysRevE.104.064205

I. INTRODUCTION

Wave instabilities play an important role in the evolution of nonlinear systems, as they are associated with symmetry-breaking effects resulting in the formation of coherent structures or leading to chaotic states [1]. A pertinent example is the modulational instability (MI) of plane waves in media governed by the focusing nonlinear Schrödinger (NLS) equation, with MI resulting in a variety of important nonlinear processes, such as the formation of envelope bright solitons, envelope shock waves, and rogue waves [2]. Another example is the transverse instability, which refers to the growth of transverse modulations of quasi-one-dimensional (1D) (stripe) bright and dark solitons, for focusing [3,4] and defocusing [5,6] NLS models, respectively. In the elliptic 2D focusing NLS, the norm of the soliton stripes is infinite, as they extend to infinity in the transverse direction. Hence, the bright soliton stripes, being subject to the onset of collapse, break up, through a width modulation, into individual 2D lump-shaped structures. In such a case, the transverse instability is of the so-called "necking" type [7]. However, bright solitons of the hyperbolic 2D focusing NLS, as well as dark solitons of the elliptic 2D defocusing NLS, undergo undulations of the location of their center, due to the transverse instability, and eventually decay; due to this so-called "snaking" instability, bright soliton stripes decay into bright lumps, while dark solitons decay into vortices or dark lumps [8,9]. It is important to note that this is a popular experimental technique for observing the instability outcome and subsequent pattern formation both in atomic physics [10] and in nonlinear optics [11,12].

Arrest or substantial suppression of the transverse instability of solitons has been proved to be a topic of great interest, and various physical mechanisms have been proposed to suppress this instability. These mechanisms include the coupling of solitons with another soliton component [13,14], making the soliton sufficiently incoherent along the transverse direction [15], as well as using periodic lattice potentials [16,17] or localized barrier potentials [18]. In addition, nonlocal nonlinearities, occurring, e.g., in plasmas [19], atomic vapors [20], lead glasses [21], nematic liquid crystals [22], as well as dipolar Bose-Einstein condensates [23], are known to play a key role on the stability of solitons. In particular, in settings with focusing nonlocal nonlinearities, the transverse instability of 1D bright nonlocal solitons can be substantially suppressed [24]. Furthermore, the catastrophic self-focusing effect in local media described by higher-dimensional NLS-type equations is suppressed by nonlocality, and it is thus absent in nonlocal media [25,26] (see also the review in Ref. [27]); as a result, stable 2D and 3D solitons can be formed [20,21,26–29]. However, in settings with defocusing nonlocal nonlinearities, the transverse instability of dark nonlocal solitons [30–33] can be suppressed [26,34].

In this work, we revisit the problem of the transverse instability and dynamics of bright solitons in nonlocal nonlinear media. The considered nonlocal NLS model, namely a Schrödinger type paraxial wave equation, coupled with a diffusion-type equation governing the nonlocal response of the medium, is relevant to a variety of physical contexts. These include optical media with a thermal nonlinearity (e.g., atomic vapors [20,21] and liquid solutions [35,36]), plasmas [19,37], and nematic liquid crystals [38,39]. The considered nonlocal NLS possesses a sech^2-shaped exact analytical bright soliton solution, which cannot be reduced—in the local nonlinearity limit—to the usual sech-shaped bright soliton of the NLS; hence, one cannot exploit this limit to study the effect of nonlocality on the transverse instability of nonlocal soliton stripes, as has been done, e.g., in Ref. [24].

Here, we analyze the problem by employing a perturbation method, similar to the one used in Ref. [40] (see also

Ref. [41]), which uses a perturbation ansatz relying on the sech^2 nonlocal soliton, with a center and a phase becoming unknown functions of slow time and transverse coordinate. We find an approximate solution of the nonlocal NLS, where the correction to the soliton shape is shown to feature an exponential growth in time, which is a signature of the transverse instability. The latter is of the necking type and is induced by the soliton phase, which is shown to obey an elliptic partial differential equation (PDE). We show that the instability growth rate (i.e., the inverse characteristic timescale associated with the exponential growth of the phase) depends on the inverse square root of the nonlocality parameter, a fact highlighting the substantial, nonlocality-induced suppression of the transverse instability of the bright soliton stripes (in a similar vein as earlier works [24]). The analytical estimation for the growth rate, as well as the derived approximate analytical solution, are found to be in good agreement with respective results obtained by means of direct simulations. Despite the prolongation of the lifetime of the solutions obtained herein, our results do not support the scenario of a complete stabilization of the relevant bright soliton stripes, irrespectively of the value of nonlocality parameter ν, for the range considered herein.

The presentation of the manuscript is organized as follows. In Sec. II, we introduce the model and its exact soliton solution and present the results of our perturbation method; these include the derivation of the evolution of the soliton parameters, the derivation of the instability growth rate, as well as the first-order correction of the soliton shape. Section III is devoted to the presentation of our numerical results and comparison with the analytical approximations. Finally, in Sec. IV we summarize our conclusions and discuss possibilities for relevant future research.

II. MODEL AND STABILITY ANALYSIS

A. The model and its exact 1D soliton solutions

We consider the propagation of an optical beam in a nonlocal nonlinear medium. Let u be the complex electric field envelope of the light beam satisfying a paraxial, Schrödinger-type equation, and the real function θ be the nonlinear, generally nonlocal, medium's response, assumed to obey a diffusion-type equation [29]. Then, the evolution of the beam is governed by the following dimensionless nonlocal NLS model:

$$iu_t + \frac{d}{2}\Delta u + 2g\theta u = 0, \tag{1}$$

$$\nu\Delta\theta - 2q\theta + 2g|u|^2 = 0, \tag{2}$$

where subscripts denote partial derivatives. Here, the evolution variable t represents the propagation distance (assumed to be along the z direction), $\Delta \equiv \partial_x^2 + \partial_y^2$ is the transverse Laplacian, while g and d are coupling and diffraction coefficients, assumed to be positive; this case corresponds to a focusing nonlinearity. In addition, $q > 0$ is a constant and, finally, the parameter ν, which measures the diffusion length (assumed to be large compared to the operating wavelength), describes the strength of nonlocality: indeed, large ν corresponds to a highly nonlocal response while in the limit $\nu \to 0$, Eqs. (1) and (2) reduce to the following NLS equation with a local cubic (Kerr-type) nonlinearity:

$$iu_t + \frac{d}{2}\Delta u + \frac{2g^2}{q}|u|^2 u = 0. \tag{3}$$

The model Eqs. (1) and (2) are relevant to a variety of nonlocal media. These include: (a) optical media featuring a thermal nonlinearity—such as atomic vapors [20,21] and liquid solutions, with θ being the nonlinear correction to the refractive index [35,36]; (b) ionized plasmas, with θ being the relative electron temperature perturbation, and $q \propto m/M$ being the relative energy that an electron of mass m delivers to a heavy particle of mass M during a single collision [19,37]; (c) nematic liquid crystals [38,39], with θ denoting the perturbation of the optical director angle from its static value due to the light beam, and q being related to the applied static field which pretilts the nematic dielectric [22,42].

It is now convenient to rescale the independent variables and the function θ in Eqs. (1) and (2), so as to reduce the number of parameters involved. For this purpose, we use the scalings

$$\mathbf{r} \mapsto \frac{g}{\sqrt{qd}}\mathbf{r}, \quad t \mapsto \frac{g^2}{q}t, \quad \theta \mapsto \frac{g}{q}\theta,$$

where $\mathbf{r} = (x, y)$, and cast Eqs. (1) and (2) into the form

$$iu_t + \frac{1}{2}\Delta u + 2\theta u = 0, \tag{4}$$

$$\nu\Delta\theta - 2\theta + 2|u|^2 = 0, \tag{5}$$

with the sole remaining parameter being the nonlocality parameter $\nu \mapsto (q^2 d/g^2)\nu$. Notice that, in the context of nematic liquid crystals, this parameter is large, taking values of the order of $O(10^2)$ [22,38,39,42]. However, for thermal nonlinear media, such as liquid solutions [35,36], as well as for partially ionized plasmas [37], the nonlocality parameter takes values in the interval $0.1 \lesssim \nu \lesssim 10$.

As explained in the Introduction, our scope is to study the transverse dynamics of 1D bright soliton stripes in the 2D setting and investigate, in particular, the role of nonlocality. It is thus convenient to start by presenting such 1D bright soliton solutions of Eqs. (4) and (5), which were first found in the pioneering work [43] (see also Ref. [44]). This bright soliton solution can be found upon using the following ansatz:

$$u = q_0(\xi)\exp[i\omega(t + \sigma_0)], \quad \theta = \theta_0(\xi), \tag{6}$$

where q_0 is an unknown real function depending on $\xi = k(x - x_0)$, k is an unknown constant, ω is the unknown frequency of the solution, while x_0 and σ_0 are arbitrary real parameters representing, respectively, the initial location and the phase of the soliton. Substituting Eqs. (6) into Eqs. (4) and (5), it can be found that the resulting equations become

$$k^2 q_{0\xi\xi} - 2\omega q_0 + 4q_0\theta_0 = 0, \tag{7}$$

$$\nu k^2 \theta_{0\xi\xi} - 2\theta_0 + 2q_0^2 = 0. \tag{8}$$

Then, observing that if

$$\theta_0 = \sqrt{\frac{1}{2\nu}}q_0, \quad \text{and} \quad \omega = \frac{1}{\nu}, \tag{9}$$

then the system Eqs. (7) and (8) reduces to a single ordinary differential equation (ODE):

$$q_{0\xi\xi} - \frac{2}{\nu k^2} q_0 + \frac{4}{\sqrt{2\nu} k^2} q_0^2 = 0. \tag{10}$$

The latter possesses the exact soliton solution

$$q_0(\xi) = \frac{3}{2\sqrt{2\nu}} \mathrm{sech}^2[k(x - x_0)], \quad k = \sqrt{\frac{1}{2\nu}}, \tag{11}$$

which implies that the soliton solutions of Eqs. (4) and (5) are of the form

$$u_0(x,t) = \frac{3}{2\sqrt{2\nu}} \mathrm{sech}^2[k(x - x_0)] \exp[i\omega(t + \sigma_0)], \tag{12}$$

$$\theta_0(x,t) = \frac{3}{4\nu} \mathrm{sech}^2[k(x - x_0)]. \tag{13}$$

Here it is interesting to note that, while the system of Eqs. (4) and (5) reduces to the local NLS Eq. (3), the exact solution Eq. (12) cannot be reduced to the soliton solution of Eq. (3) (which features a sech-profile and is characterized by a free parameter); this becomes clear by the fact that $\lim_{\nu\to 0} u_0 \to \infty$. It is also mentioned that Eqs. (12) and (13) represent a stationary solution of the problem; traveling solutions exist as well and can easily be constructed by means of a Galilean boost.

B. Perturbation theory

In order to study the stability of solutions of Eqs. (12) and (13) in two dimensions, we consider solutions of Eqs. (4) and (5) in the form of the following asymptotic expansions:

$$u(\xi, t, T_i, Y_i) = \sum_{j=0}^{\infty} \epsilon^j q_j(\xi) \exp\{i\omega[t + \sigma_0(T_i, Y_i)]\}, \tag{14}$$

$$\theta(\xi, T_i, Y_i) = \sum_{j=0}^{\infty} \epsilon^j \theta_j(\xi, T_i, Y_i), \tag{15}$$

$$\xi = k[x - x_0(T_i, Y_i)], \tag{16}$$

where $T_i = \epsilon^i t$, $Y_i = \epsilon^i y$ and $0 < \epsilon \ll 1$ is a formal small parameter. The above perturbation ansatz is actually inspired by the form of the exact solution of Eq. (6) of the 1D problem but, now, with the soliton's center x_0 and phase σ_0 becoming unknown functions of the slow variables T_i and Y_i. Substituting the perturbation expansions Eqs. (14) and (15) into Eqs. (4) and (5) we obtain the following results.

First, at $O(\epsilon^0)$, we obtain the system of Eqs. (7) and (8), which provides the exact soliton solution of Eq. (11) [that eventually leads, together with Eq. (9), to the solution of Eqs. (12) and (13)].

At the next orders of approximation, the presence of derivatives of x_0 and σ_0 with respect to the slow variables renders the inhomogeneous parts F_j of the resulting equations for q_j (with $j = 1, 2, \ldots$) complex, i.e., $F_j = F_j^{(\mathrm{r})} + iF_j^{(\mathrm{i})}$; this implies that q_j itself must be complex, i.e., $q_j = q_j^{(\mathrm{r})} + iq_j^{(\mathrm{i})}$. Thus, separating real and imaginary parts of the resulting equations, we obtain, at each order, a set of three equations, two of which are coupled. To be more specific, the resulting equations at orders $O(\epsilon^j)$ for $j = 1, 2, \ldots$ take the following form:

$$\left(k^2\partial_\xi^2 - 2\omega + 4\theta_0\right) q_j^{(\mathrm{r})} + 4q_0\theta_j = F_j^{(\mathrm{r})}, \tag{17}$$

$$\left(k^2\partial_\xi^2 - 2\omega + 4\theta_0\right) q_j^{(\mathrm{i})} = F_j^{(\mathrm{i})} \tag{18}$$

$$\left(\nu k^2\partial_\xi^2 - 2\right)\theta_j + 4q_0 q_j^{(\mathrm{r})} = G_j. \tag{19}$$

The inhomogeneous parts at the order $O(\epsilon)$ are given by

$$F_1^{(\mathrm{r})} = 2\omega\sigma_{0T_1} q_0, \quad F_1^{(\mathrm{i})} = 2kx_{0T_1} q_{0\xi}, \quad G_1 = 0, \tag{20}$$

while at the order $O(\epsilon^2)$ they read

$$\begin{aligned} F_2^{(\mathrm{r})} = &- 4q_1^{(\mathrm{r})}\theta_1 - k^2 x_{0Y_1}^2 q_{0\xi\xi} + kx_{0Y_1Y_1} q_{0\xi} \\ &+ \omega^2\sigma_{0Y_1}^2 q_0 + 2\omega\sigma_{0T_2} q_0 + 2\omega\sigma_{0T_1} q_1^{(\mathrm{r})} \\ &+ 2q_{1T_1}^{(\mathrm{i})} - 2\nu x_{0T_1} q_1^{(\mathrm{i})}, \end{aligned} \tag{21}$$

$$\begin{aligned} F_2^{(\mathrm{i})} = &- 4q_1^{(\mathrm{i})}\theta_1 + 2k\omega x_{0Y_1}\sigma_{0Y_1} q_{0\xi} - \omega\sigma_{0Y_1Y_1} q_0 \\ &+ 2kx_{0T_2} q_{0\xi} + 2\omega\sigma_{0T_1} q_1^{(\mathrm{i})} - 2q_{1T_1}^{(\mathrm{r})} \\ &+ 2kx_{0T_1} q_{1\xi}^{(\mathrm{r})}, \end{aligned} \tag{22}$$

$$G_2 = -\nu k^2 x_{0Y_1}^2 \theta_{0\xi\xi} + \nu k x_{0Y_1Y_1}\theta_{0\xi} - 2\left(q_1^{(\mathrm{r})2} + q_1^{(\mathrm{i})2}\right). \tag{23}$$

To proceed further, it is useful to make a few observations. First, differentiating Eqs. (7) and (8) with respect to ξ, one obtains the homogeneous part of Eqs. (17)–(19). This implies that the homogeneous solutions of Eqs. (17)–(19) are of the form

$$q_{jh}^{(\mathrm{r})} = q_{0\xi}, \quad q_{jh}^{(\mathrm{i})} = q_0, \quad \theta_{jh} = \theta_{0\xi}. \tag{24}$$

Second, having found the above homogeneous solutions, we may derive the solvability conditions of the full inhomogeneous problem, Eqs. (17)–(19). To do this, first we consider the coupled Eqs. (17) and (19). We multiply both sides of Eqs. (17) by the homogeneous solution $q_{jh}^{(\mathrm{r})}$, as well as both sides of Eq. (19) by the homogeneous solution θ_{jh}. Then, we add the resulting equations and integrate with respect to ξ from $-\infty$ to $+\infty$. This yields the following integral relation:

$$\int_{-\infty}^{\infty} \left(q_{jh}^{(\mathrm{r})} F_j^{(\mathrm{r})} + \theta_{jh} G_j\right) d\xi = 0, \tag{25}$$

which is the solvability condition of Eqs. (17) and (19). To obtain the solvability condition for Eq. (18), we follow a similar procedure, namely, we multiply both sides of Eq. (18) by the homogeneous solution $q_{jh}^{(\mathrm{i})}$ and integrate from $-\infty$ to $+\infty$; this yields

$$\int_{-\infty}^{\infty} q_{jh}^{(\mathrm{i})} F_j^{(\mathrm{i})} d\xi = 0. \tag{26}$$

Importantly, the above solvability conditions will lead to evolution equations for the soliton center x_0 and phase σ_0 which—as we will see—will provide the necessary information for characterizing the stability of the 1D soliton solutions. Furthermore, solving Eqs. (17)–(19) (for $j = 1$) will provide us the form of the solution to Eqs. (4) and (5) up to $O(\epsilon)$, and for short times—up to the onset of the instability. This will be particularly relevant for our direct numerical simulations as well.

C. Evolution of the soliton parameters

First we consider the problem at the order $O(\epsilon)$. In this case, the solvability conditions, Eqs. (25) and (26) lead to the following results, respectively:

$$\int_{-\infty}^{\infty} q_{0\xi}(2\omega\sigma_{0T_1}q_0)d\xi = 2\omega\sigma_{0T_1}\int_{-\infty}^{\infty}(q_0q_{0\xi})d\xi = 0 \quad (27)$$

and

$$\int_{-\infty}^{\infty} q_0(2kx_{0T_1}q_{0\xi})d\xi = 2kx_{0T_1}\int_{-\infty}^{\infty}(q_0q_{0\xi})d\xi = 0. \quad (28)$$

The above results indicate that the solvability conditions at this order, $O(\epsilon)$, are always satisfied, regardless of the specific form of the soliton parameters x_0 and σ_0. Thus, we may proceed by solving Eqs. (17)–(19) (see details for the derivation of these solutions in the Appendix), and find the following exact solutions for the soliton correction q_1:

$$q_1^{(\mathrm{i})} = \frac{3}{2}x_{0T_1}\xi\,\mathrm{sech}^2(\xi), \quad (29)$$

$$q_1^{(\mathrm{r})} = -\frac{3}{16\sqrt{2\nu}}\sigma_{0T_1}\mathrm{sech}^3(\xi)[-9\cosh(\xi) + \cosh(3\xi) + 12\xi\sinh(\xi)]. \quad (30)$$

Notice that $q_1^{(\mathrm{r})} \to -\frac{3}{16\sqrt{2\nu}}\sigma_{0T_1}$ as $|\xi| \to \infty$, a fact that is associated with the emergence of a *shelf*, i.e., a linear wave adjacent to the soliton. Shelves were first found in the context of perturbed Korteweg-de Vries (KdV) equations [41] and later were also studied for both focusing [45] and defocusing [46] NLS models with a local nonlinearity. Generally, the emergence of shelves leads to the breakdown of the perturbation theory at a higher order approximation in the perturbation scheme [41]. While this issue, along with the appearance of the shelf, are interesting by themselves, they will not be considered here; in our case, the instability induced by the presence of σ_{0T_1} in Eq. (30) (see below) plays the dominant role in the evolution of the soliton.

To proceed further, we apply the solvability condition at $O(\epsilon^2)$, in which case Eqs. (25) and (26), respectively, read

$$\int_{-\infty}^{\infty}\left[q_{0\xi}\left(kx_{0Y_1Y_1}q_{0\xi} + 2\omega\sigma_{0T_2}q_0 + 2q_{1T_1}^{(\mathrm{i})}\right) + \theta_0(\nu kx_{0Y_1Y_1}\theta_{0\xi})\right]d\xi = 0$$
$$\Rightarrow x_{0T_1T_1} - \frac{3}{5\nu}x_{0Y_1Y_1} = 0 \quad (31)$$

and

$$\int_{-\infty}^{\infty}\left[q_0\left(-\omega\sigma_{0Y_1Y_1}q_0 + 2kx_{0T_2}q_{0\xi} - 2q_{1T_1}^{(\mathrm{r})}\right)\right]d\xi = 0$$
$$\Rightarrow \sigma_{0T_1T_1} + \frac{4}{3\nu}\sigma_{0Y_1Y_1} = 0. \quad (32)$$

The set of Eqs. (31) and (32), which is one of the main results of our analytical approach, must be satisfied in order for our original system of Eqs. (17)–(19) to be solvable, up to the order $O(\epsilon^2)$. We note that, in the above equations, no nonlinear terms in x_0 [in Eq. (31)] and σ_0 [in Eq. (32)] are involved, since such terms vanish when applying the solvability condition; thus, Eqs. (31) and (32) do not involve any approximations, up to this order of approximation.

Evidently, Eq. (31) is a hyperbolic PDE (having the form of the usual second-order wave equation) and, thus, its solutions corresponding to bounded initial data never blow up. On the contrary, Eq. (32) is an elliptic PDE (of the Laplace type) and, thus, any bounded initial condition features an exponential growth. As a consequence, the exponential growth of σ_0 will result in an exponential growth of $q_1^{(\mathrm{r})}$ as indicated by Eq. (30); in other words, any initial condition of the form Eqs. (12) and (13) is unstable in the 2D setting. Notice that the fact that $x_0(Y_1, T_1)$ obeys a hyperbolic PDE, while $\sigma_0(Y_1, T_1)$ obeys an elliptic PDE, bears resemblance to the case of the instability of bright soliton stripes of the elliptic NLS equation, with local cubic nonlinearity in $(2+1)$-dimensions [9,41].

D. Instability and instability growth rate

To investigate the instability-induced soliton dynamics, first we note that, in practice, the instability is anticipated to manifest itself at finite time. This means that there exists a characteristic timescale τ for the manifestation of the instability leading the bright soliton stripe to decay into purely 2D structures (similarly to the case of the elliptic 2D NLS [9]). To calculate this timescale, we need to consider some specific initial conditions for the PDEs (31) and (32). In particular, without loss of generality, we supplement Eq. (31) with the following initial data

$$x_0(0, Y_1) = \delta\cos(KY_1), \quad x_{0T_1}(0, Y_1) = 0, \quad (33)$$

and Eq. (32) with the initial data

$$\sigma_0(0, Y_1) = \delta\cos(KY_1), \quad \sigma_{0T_1}(0, Y_1) = 0, \quad (34)$$

where δ and K represent the perturbation amplitude and wavenumber, respectively. Then, the solutions of Eqs. (31) and (32) take, respectively, the following form:

$$x_0(T_1, Y_1) = \frac{\delta}{2}\left\{\cos\left[K\left(Y_1 - \sqrt{\frac{3}{5\nu}}T_1\right)\right] + \cos\left[K\left(Y_1 + \sqrt{\frac{3}{5\nu}}T_1\right)\right]\right\}, \quad (35)$$

$$\sigma_0(T_1, Y_1) = \frac{\delta}{2}\left[\exp\left(K\sqrt{\frac{4}{3\nu}}T_1\right)\cos(KY_1) + \exp\left(-K\sqrt{\frac{4}{3\nu}}T_1\right)\cos(KY_1)\right]. \quad (36)$$

Obviously, Eq. (35) represents the usual D'Alembert solution composed by a right- and a left-going wave; this solution is always bounded and never grows. This, however, is not the case of the solution Eq. (36), which grows exponentially. In fact, it can be inferred from Eq. (36) that the solution grows in time as $\sigma_0 \propto \exp(t/\tau)$, where the characteristic timescale τ is given by

$$\tau = \frac{1}{\Gamma} \equiv \frac{1}{\epsilon K\sqrt{\frac{4}{3\nu}}} = \frac{\sqrt{3}}{2\epsilon K}\sqrt{\nu}, \quad (37)$$

with $\Gamma = 1/\tau$ being the instability growth rate. It is important to point out that Eq. (37) reveals that, for fixed ϵ and K, the characteristic time τ scales according to the $\sqrt{\nu}$ law,

meaning that the instability manifests itself for longer times as the nonlocality becomes stronger. As mentioned in the Introduction, suppression of instabilities is a generic feature of nonlocality; this occurs in our case as well, but the transverse instability of the bright soliton stripe cannot be completely arrested. Nevertheless, strong nonlocality (i.e., large ν) is able to significantly prolong the soliton lifetime.

To further quantify the above results, and as a preamble for our numerical simulations, it is now convenient to write down the soliton solution, up to $O(\epsilon)$, namely,

$$u(x,y,t) = u_0(\xi) + \epsilon u_1(\xi, T_1, Y_1) + O(\epsilon^2),$$

with $\xi = k[x - x_0(T_1, Y_1)]$. Substituting Eqs. (29), (30), and (12) into the expression above the soliton solution takes the form

$$u(x,y,t) = \left\{ \frac{3}{2\sqrt{2\nu}} \mathrm{sech}^2(\xi) + \epsilon \left[-\frac{3}{16\sqrt{2\nu}} \sigma_{0T_1} \times \mathrm{sech}^3(\xi)(-9\cosh(\xi) + \cosh(3\xi) + 12\xi \sinh(\xi)) + i\frac{3}{2} x_{0T_1} \xi \mathrm{sech}^2(\xi) \right] \right\} \times \exp[i\omega(t + \sigma_0)] + O(\epsilon^2), \quad (38)$$

with ω given in Eq. (9). It is now clear that the soliton solution $u(x,y,t)$ grows exponentially due to the presence of the term σ_{0T_1} and eventually will break up. In the next section, we will present numerical results to study the instability dynamics, check the validity of the solution of Eq. (38), as well as the estimation for the growth rate [Eq. (37)] against direct numerical simulations.

III. NUMERICAL RESULTS

We now proceed with results obtained by means of dynamical simulations of the system's evolution. The latter are performed by numerically integrating Eqs. (4) and (5) using a high accuracy spectral method [47]. The initial condition is borrowed from the soliton solution of Eq. (38), for $t = 0$, using the initial conditions of Eqs. (33) and (34). In particular, the initial condition for the field u is taken to be

$$u(x,y,0) = \left(\frac{3}{2\sqrt{2\nu}} \mathrm{sech}^2\{k[x - \delta\cos(\epsilon K y)]\} \right) \times \exp[i\omega\delta\cos(\epsilon K y)]. \quad (39)$$

It is clear that the terms $\propto\delta$ above describe small perturbations in the initial soliton center position and phase, while the argument of the soliton's phase, which is $\propto\epsilon$, implies that the relevant perturbation is a long-wavelength one.

The parameter values used in the simulations are

$$K = 3, \quad \epsilon = \delta = 0.1, \quad (40)$$

while the nonlocality parameter ν was varied in the interval [1,20]; such values of ν are relevant to thermal nonlinear media, such as liquid solutions [35,36], and partially ionized plasmas [37]. Notice that both ϵ and δ, which were considered as small parameters in our perturbation scheme, were assumed to take relatively large values; nevertheless, as we will see, even for such a choice, the analytical results are found to be in good agreement with the results of the simulations. It is also noticed that other choices for the rest of the parameter values led to results qualitatively similar to the ones that will be presented below.

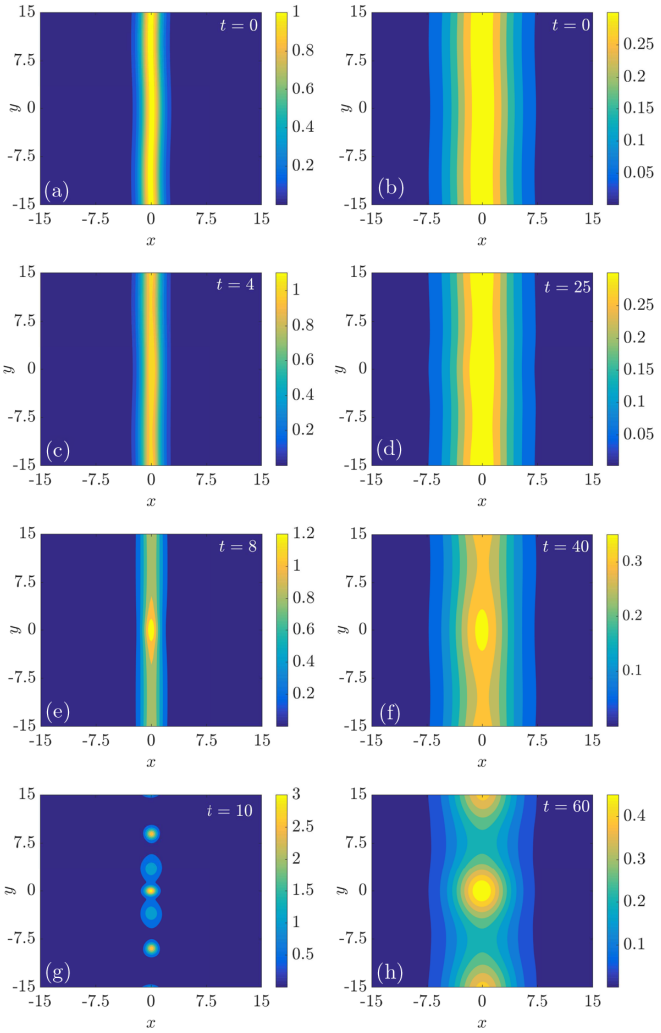

FIG. 1. Contour plots showing the evolution of the soliton modulus, $|u(x,y,t)|$, for $\nu = 1$ (left panels) and $\nu = 10$ (right panels); in addition, $\delta = 0.1$, and other parameter values are given in Eq. (40). Panels (a) and (b) show the initial condition [Eq. (39) for $t = 0$], while the other panels show characteristic snapshots of u. Eventually, the soliton decays into a chain of 2D structures (see also Fig. 2).

First, we present results showcasing the instability-induced dynamics of solitons. In Fig. 1, we show contour plots depicting the evolution of the soliton modulus, $|u(x,y,t)|$, for different times. In the left panels we use the value of the nonlocality parameter $\nu = 1$, while in the right panels we showcase the larger nonlocality strength of $\nu = 10$; other parameter values are given in Eq. (40). Figures 1(a) and 1(b) show the initial condition ($t = 0$), as given in Eq. (39), while the other panels show characteristic snapshots of u for $t \neq 0$; observe that for the weaker nonlocality ($\nu = 1$), the soliton width, $1/k$ [with k given in Eq. (11)], is shorter.

As is clearly seen, in both cases, the soliton stripes are prone to the instability, which is of the necking type [7].

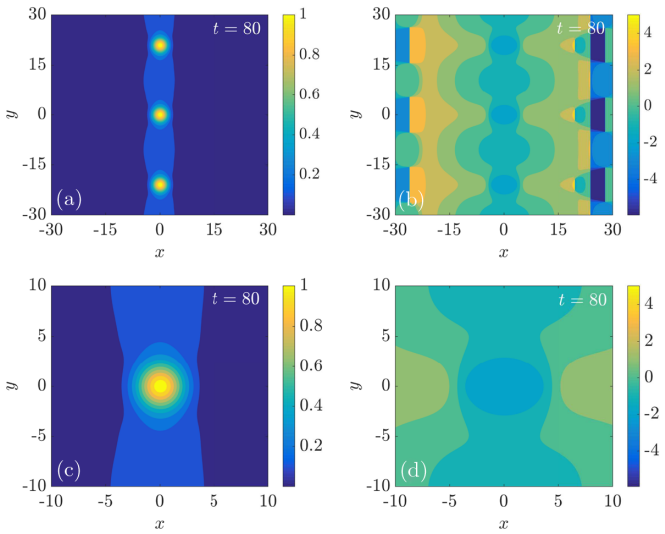

FIG. 2. Contour plots showing the modulus (a) and the phase (b) of $u(x, y, t)$ at $t = 80$, for nonlocality parameter $\nu = 10$; other parameters are kept fixed, as given in Eq. (40). This state consists of a chain of vorticity-free 2D structures, as is also seen in the bottom zoom (c), (d).

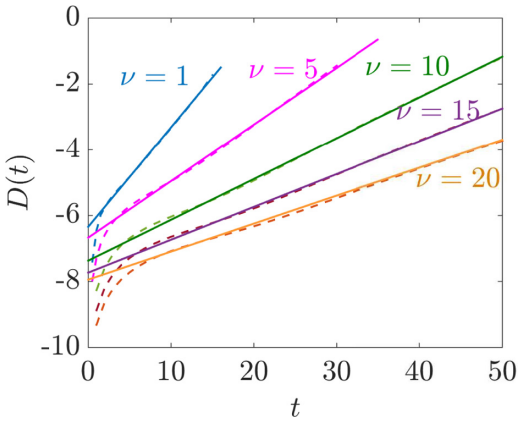

FIG. 3. The logarithm of the modulus of the difference $D(t)$ [see Eq. (41)] as a function of time, for different values of the nonlocal parameter ν; here, $u_{\rm num}$ is the numerical solution, and u_0 is the exact analytical soliton solution. The dashed lines correspond to the numerical results for each value of ν, while the solid lines to their corresponding linear fits (once the instability sets in and, indeed, after an initial transient stage). The latter are in good agreement with the predicted growth rates of Eq. (37) (see Table I).

Nevertheless, the soliton in the setting with $\nu = 10$ (right panels) takes a longer time to break up. Hence, nonlocality leads to a substantial suppression of the transverse instability of the soliton stripes, similarly to what was found for the branch of solutions arising from the standard local NLS soliton of $\nu = 0$ in Ref. [24]. However, it is seen that eventually, in either case, the solitons decay into a chain of 2D localized structures, as is also shown in Fig. 2; there, the modulus and the phase of such a chain is depicted at $t = 80$, for a nonlocality parameter of $\nu = 10$. Notice that the phase profile of the emerging 2D structures, depicted in the right panel of the figure, show that these waveforms are long-lived, vorticity-free ones.

At this point, it should also be pointed out that Figs. 2(c) and 2(d) clearly indicate the saturation of the transverse instability into a (chain of) "solitonic" 2D structure(s). This is in accordance with the analysis of Ref. [26], where it is rigorously proved that nonlocality eliminates collapse in higher dimensions, for a nonlocal response function with a positive definite Fourier spectrum, as is our case [48]. Thus, the saturation of the transverse instability of the soliton stripe is actually due to the suppression of the self-focusing effect in nonlocal media. Notice that, for the local case, it was demonstrated by higher-order perturbations that the transverse instability will lead to self-focusing "blobs" [49]. It would be thus interesting to follow an analysis similar to that of Ref. [49] in the nonlocal case under consideration. However, such an analysis is beyond the scope of this work.

Next, it is relevant to test the validity of the analytical estimation for the growth rate $\Gamma = 1/\tau$, with τ given by Eq. (37). To do this, in Fig. 3, we show the logarithm of the modulus of the difference

$$D(t) = \log |u_{\rm num}(0, 0, t) - u_0(0, 0, t)|, \qquad (41)$$

where $u_{\rm num}$ is the numerical solution and u_0 is the exact analytical soliton solution [see Eq. (12)], evaluated at $x = 0$, $y = 0$, as a function of time; shown are curves corresponding to different nonlocality parameters, namely, $\nu = 1$, $\nu = 5$, $\nu = 10$, $\nu = 15$, and $\nu = 20$. The idea here is that, subtracting the exact soliton solution from the numerical one, one seeks to isolate the predicted exponential growth of the soliton correction, and investigate whether it agrees with the analytical prediction of $\exp(t/\tau)$ dependence.

The numerical results, depicted by the dashed curves, show that at the early stage of the evolution ($t \lesssim 2$ for $\nu = 1$ up to $t \lesssim 7$ for $\nu = 20$), the considered function undergoes a transient stage until the instability gets activated. Once the latter activation materializes, the relevant plot of the logarithmic diagnostic of choice features a linear growth. This is obviously a signature of the exponential growth of the solution that was predicted above, while the slopes of the pertinent straight lines should correspond to the growth rates for the different values of ν [see Eq. (37)]. Indeed, the slopes of the relevant linear fits (solid lines) are close to the analytically predicted growth rates $\Gamma = 1/\tau$ for each value of ν, as shown in Table I. As seen in the table, the resulting relative error between the numerical result and the analytical prediction ranges between 8% to 12%, for all considered values of ν, signaling the good agreement between the two.

TABLE I. Comparison between the slopes of the linear fits of the numerical data of Fig. 3 and the analytical prediction for the growth rate, $\Gamma = 1/\tau$, for various values of ν.

ν	Linear fit slope	$\Gamma = 1/\tau$	Approximate % error
1	0.38	0.35	8
5	0.17	0.15	10
10	0.12	0.11	9
15	0.10	0.09	10
20	0.09	0.08	12

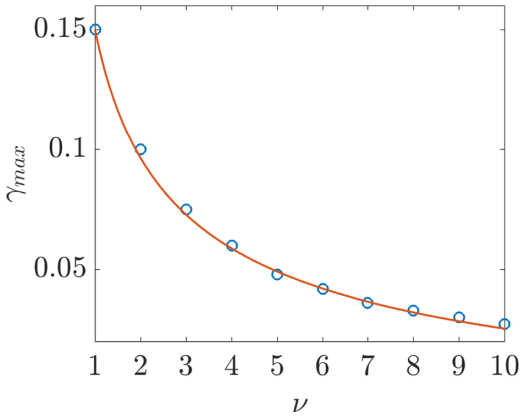

FIG. 4. The maximum growth rate γ [see Eq. (43)] as a function of the nonlocality parameter ν. Here, (blue) circles correspond to the numerical results, while the (red) solid line is the best fit corresponding to a curve $\propto 1/\sqrt{\nu}$ (see text).

We note in passing that we have also compared the above results, relying on the use of the local parameter $D(t)$, with an averaged growth rate $\bar{D}(t)$ integrated over the spatial coordinates x and y, namely,

$$\bar{D}(t) = \frac{1}{L^2}\int_{-\frac{L}{2}}^{\frac{L}{2}}\int_{-\frac{L}{2}}^{\frac{L}{2}} \log|u_{\rm num}(x,y,t) - u_0(x,y,t)|dxdy, \tag{42}$$

where $L \times L$ is our computational domain (here, we use $L = 30$). We found that the time-dependence of $\bar{D}(t)$ is almost identical to the one of $D(t)$, modulo a displacement (results not shown here); this displacement, is expected by the fact that $\bar{D}(0) \neq D(0)$.

We have also calculated numerically the growth rate $\gamma(t)$, as defined in Refs. [50,51], namely,

$$\gamma(t) = \frac{1}{2\Delta t}\ln\left[\frac{N(t+\Delta t)}{N(t)}\right], \tag{43}$$

where Δt is the time step (here, we use $\Delta t = 0.5$) and

$$N(t) = \int_{-\frac{L}{2}}^{\frac{L}{2}}\int_{-\frac{L}{2}}^{\frac{L}{2}} |u_1(x,y,t)|^2 dxdy,$$

is the norm of the soliton correction (i.e., of the soliton's perturbation). The result for the maximum value $\gamma_{\rm max}$ of $\gamma(t)$ is shown in Fig. 4 as a function of the nonlocality parameter ν, for $\nu \in [1, 10]$. The maximum growth rate $\gamma_{\rm max}$ was determined for each value of ν as follows: we numerically calculated $\gamma(t)$, and then found its maximum value, which was obtained after an initial transient stage, similarly to the situation observed in Fig. 3. In Fig. 4, the numerical result for $\gamma_{\rm max}$ [(blue) circles] is compared with the best fit with the function $A\nu^p + B$ [solid (red) line]; this corresponds to $p = -0.5$, $A = 0.1814$, and $B = -0.032$. It can readily be observed that the maximum growth rate clearly follows the $1/\sqrt{\nu}$ law that was analytically predicted in the previous Section. Hence, given that the maximum growth decreases as $1/\sqrt{\nu}$, the transverse instability of the bright soliton stripe is suppressed according to this law.

It is also relevant to provide an additional test for the validity of our analytical result concerning the solution given in Eq. (38), against results of the numerical simulations. In Fig. 5, solid (white) isocontour lines of constant modulus, corresponding to the approximate analytical solution Eq. (38), are "superimposed" on top of contour plots showing the modulus of the numerical solution, for $\nu = 1$. In Figs. 5(a)– 5(d), corresponding to $t = 2, 4, 6, 8$, a qualitative agreement between the numerical and the analytical solution is observed, especially around the soliton maximum. Naturally, discrepancies occur at the soliton tails as contributions beyond our analysis of $O(\epsilon)$ [such as, e.g., ones at $O(\epsilon^2)$] become progressively more important. Notice that the discrepancy between the numerical and the analytical solution becomes larger as time increases, due to the exponential growth of the instability, which is only captured via the $O(\epsilon)$ terms in the approximate analytical solution of Eq. (38). Finally, and as is naturally expected, past the time $t = 8$ [Fig. 5(d)], the analytical result fails, as the soliton has already been destroyed.

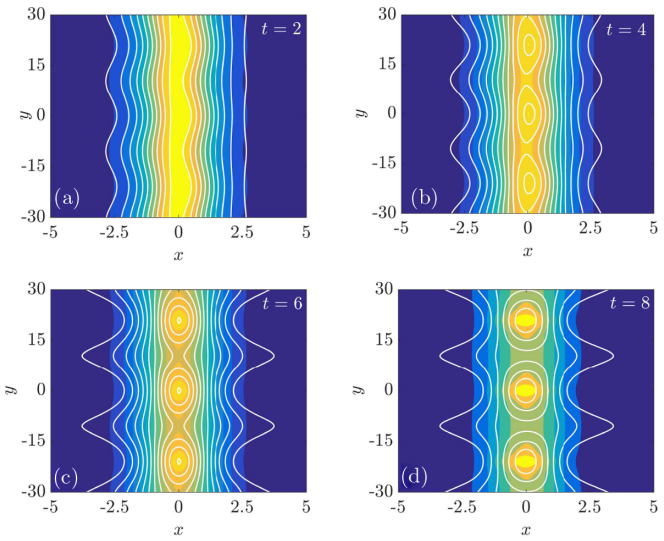

FIG. 5. Solid (white) isocontour lines of constant modulus, corresponding to the analytical solution Eq. (38), are "superimposed" on top of contour plots showing the modulus of the numerical solution, for $t = 2, 4, 6, 8$, and for $\nu = 1$.

IV. CONCLUSIONS

In this work, we studied the transverse dynamics and, in particular, the transverse instability of bright soliton stripes in media with a spatially nonlocal nonlinear response. The considered nonlocal nonlinear Schrödinger (NLS) model describes beam propagation in different types of nonlocal nonlinear media, including thermal media, plasmas, and nematic liquid crystals.

Starting with an exact 1D bright soliton solution of the system (which, however, had no analog in the (local) case of nonlocality parameter $\nu = 0$), we employed a direct multiscale perturbation method to study the transverse dynamics of solitons. Assuming that the soliton's center x_0 and phase σ_0 become functions of a slow time $T_1 = \epsilon t$ and a slow transverse coordinate $Y_1 = \epsilon y$ (with $0 < \epsilon \ll 1$), we found the following. First, x_0 and σ_0 obey, respectively, a hyperbolic and an elliptic second-order PDE (with respect to T_1 and Y_1), namely, a second-order wave equation and a Laplace-type equation. The

solution of these evolution equations, together with the solution for the first-order correction to the soliton shape, led to an approximate solution of the original nonlocal NLS model, valid up to $O(\epsilon)$. It was found that the transverse instability, caused by the exponential growth of the phase σ_0, is of the necking type, and leads to the breakup of soliton stripes. The instability growth rate was found to scale with the nonlocality parameter ν according to the law $1/\sqrt{\nu}$. This fact indicates the nonlocality-induced suppression (but not full arrest) of the transverse instability of the bright soliton stripes, in line with results for different solitonic structures (bearing a $\nu = 0$ limit) within the model, as reported in previous works [24].

Direct numerical simulations were found to be in good agreement with the analytical predictions. As concerns the analytically found instability growth rate, it was shown that it is in good agreement with the numerical one (past an initial transient stage), for values of the nonlocality parameter in the interval $1 \leqslant \nu \leqslant 20$. In fact, the relative percentage error between pertinent analytical and numerical results was found to be around 10% for all the cases that were considered. Furthermore, we have also calculated the averaged growth rate γ, as defined in Refs. [50,51], as a function of the nonlocality parameter ν. We found that, for moderate values of ν [in the interval (6,15)], γ clearly follows the $1/\sqrt{\nu}$ law that was predicted analytically.

In addition, the approximate analytical soliton solution [valid up to $O(\epsilon)$] was found to follow the numerical one, with the agreement between the two being better near the the soliton center. The discrepancy between the two, especially near the soliton tails and at later times, was attributed to the fact that our analytical approximation cannot capture higher-order effects [of order $O(\epsilon^j)$, with $j \geqslant 2$], and it completely fails after the initial solitonic stripe deforms into a sequence of two-dimensional (nonvortical) solitonic "blobs."

Our work paves the way for interesting future studies. For instance, our perturbative approach could also be applied in the case of a defocusing nonlocal nonlinearity, which supports dark solitons, both in 1D [30–33] and 2D [52–54]. In such a defocusing setting, it would be interesting to study analytically the suppression of the transverse (snaking) instability of dark soliton stripes (see relevant numerical results in Ref. [34]). Furthermore, the analytical study of the transverse dynamics of solitons in multicomponent nonlocal systems (see, e.g., Ref. [55]) is another interesting and relevant theme. This is due to the fact that that there exists a plethora of vector solitons in such settings [56–58], while studies on the transverse dynamics of solitons are mainly numerical ones [59]. It would, therefore, be particularly interesting to investigate the combined effect of nonlocality and soliton coupling on the soliton instability dynamics. Finally, it would be interesting to investigate the possibility of—and conditions for—complete stabilization of the stripe soliton structures in nonlocal media. Such studies are in progress and relevant results will be reported elsewhere.

ACKNOWLEDGMENT

This material is based upon work supported by the US National Science Foundation under Grants No. PHY-2110030 (P.G.K.).

APPENDIX: SOLUTION OF $O(\epsilon)$ PERTURBATION EQUATIONS

Here, we provide a solution of the system of Eqs. (17)–(19), at the order $O(\epsilon)$ (i.e., for $j = 1$). As is observed, Eq. (18) is decoupled from Eqs. (17) and (19) and can be solved separately. Having found the solution of the homogeneous equation, $q_{1h}^{(\mathrm{i})} = q_0$ [see Eq. (24)], we seek for the solution of the full, inhomogeneous, equation in the form

$$q_1^{(\mathrm{i})}(\xi, T_1, Y_1) = q_0(\xi) f(\xi, T_1, Y_1), \tag{A1}$$

where $f(\xi)$ is an unknown function, to be determined. Substituting Eq. (A1) into Eq. (18), and employing the reduction of order method, we find

$$q_1^{(\mathrm{i})} = q_0 \Bigg[\int \frac{1}{q_0^2} \Big(\int \frac{1}{k^2} q_0 F_1^{(\mathrm{i})} d\xi \Big) d\xi + \int \frac{A_1(T_1, Y_1)}{q_0^2} d\xi + A_2(T_1, Y_1) \Bigg], \tag{A2}$$

where A_1 and A_2 are unknown functions of the slow variables T_1 and Y_1. Next, imposing the boundary condition $q_1^{(\mathrm{i})} \to 0$ as $\xi \to \pm\infty$, we obtain $A_1(T_i, Y_i) = 0$ and we choose, without loss of generality, $A_2(T_i, Y_i) = 0$ too; indeed, the term involving A_2 is of the form $\epsilon A_2(T_i, Y_i) q_0$ in the asymptotic expansion and can be absorbed in the $O(1)$ solution. This way, upon performing the relevant integrations, we derive from Eq. (A2) the solution Eq. (29).

The next step is to solve the system of Eqs. (17) and (19). To do so, first we solve Eq. (17) for the field θ_1 and find

$$\theta_1 = \frac{1}{6\sqrt{2\nu}} \Bigg\{ 3\sqrt{\frac{2}{\nu}} \sigma_{0T_1} + [-6 + 4\cosh^2(\xi)] q_1^{(\mathrm{r})} - \cosh^2(\xi) q_{1\xi\xi}^{(\mathrm{r})} \Bigg\}, \tag{A3}$$

where we have substituted the expression q_0 from Eq. (11). Obviously, once $q_1^{(\mathrm{r})}$ is found (see below), Eq. (A3) can be used for the determination of θ_1.

Next, we substitute Eq. (A3) into Eq. (19), and using the expressions for θ_0 and q_0 from Eqs. (13) and (11), we find the following fourth-order ODE for $q_1^{(\mathrm{r})}$:

$$q_{1\xi\xi\xi\xi}^{(\mathrm{r})} + 4\tanh(\xi) q_{1\xi\xi\xi}^{(\mathrm{r})} - 4[1 - \mathrm{sech}^2(\xi)] q_{1\xi\xi}^{(\mathrm{r})} - 16\tanh(\xi) q_{1\xi}^{(r)} - [16\mathrm{sech}^2(\xi) + 72\mathrm{sech}^4(\xi)] q_1^{(\mathrm{r})} + 12\sqrt{\frac{2}{\nu}} \sigma_{0T1} \mathrm{sech}^2(\xi) = 0. \tag{A4}$$

To solve the above equation, first we note that a homogeneous solution of Eq. (A4) is $q_{0\xi}$ [see Eq. (24)]. Furthermore, we can deduce that via a variation of constants method that $q_{0\xi} \int (1/q_{0\xi}^2) d\xi$ is another homogeneous solution of Eq. (A4). Having at hand two homogeneous solutions, we introduce the

following transformation:

$$q_1^{(\mathrm{r})}(\xi) = \left(q_{0\xi}\int \frac{1}{q_{0\xi}^2}d\xi\right)\left(\int q_{0\xi}w(\xi)d\xi\right) - q_{0\xi}\int\left(q_{0\xi}\int\frac{1}{q_{0\xi}^2}d\xi\right)w(\xi)d\xi, \quad \text{(A5)}$$

where $w(\xi)$ is an unknown function to be determined. Substituting Eq. (A5) into Eq. (A4) we obtain the following second-order ODE for $w(\xi)$:

$$w_{\xi\xi} + 4\tanh(\xi)w_\xi - 8\mathrm{sech}^2(\xi)w + 12\sqrt{\frac{2}{\nu}}\sigma_{0T_1}\mathrm{sech}^2(\xi) = 0. \quad \text{(A6)}$$

It is easy to check that a partial solution of Eq. (A6) is

$$w(\xi) = \frac{3}{2}\sqrt{\frac{2}{\nu}}\sigma_{0T_1}. \quad \text{(A7)}$$

Finally, substituting Eq. (A7) back to Eq. (A5), we derive the solution for $q_1^{(r)}(\xi)$, namely, Eq. (30).

[1] E. Infeld and G. Rowlands, *Nonlinear Waves, Solitons, and Chaos* (Cambridge University Press, Cambridge, UK, 1990).

[2] V. E. Zakharov and L. A. Ostrovsky, Modulation instability: The beginning, Physica D **238**, 540 (2009).

[3] V. E. Zakharov and A. M. Rubenchik, Instability of waveguides and solitons in nonlinear media, Sov. Phys. JETP **38**, 494 (1974).

[4] S. J. Han, Stability of envelope waves, Phys. Rev. A **20**, 2568 (1979).

[5] E. A. Kuznetsov and S. K. Turitsyn, Instability and collapse of solitons in media with a defocusing nonlinearity, Sov. Phys. JETP **67**, 1583 (1988).

[6] D. E. Pelinovsky, Yu. A. Stepanyants, and Yu. S. Kivshar, Self-focusing of plane dark solitons in nonlinear defocusing media, Phys. Rev. E **51**, 5016 (1995).

[7] E. A. Kuznetsov, A. M. Rubenchik, and V. E. Zakharov, Soliton stability in plasmas and hydrodynamics, Phys. Rep. **142**, 103 (1986).

[8] Yu. S. Kivshar and D. E. Pelinovsky, Self-focusing and transverse instabilities of solitary waves, Phys. Rep. **331**, 117 (2000).

[9] J. Yang, *Nonlinear Waves in Integrable and Nonintegrable Systems* (SIAM, Philadelphia, PA, 2010).

[10] B. P. Anderson, P. C. Haljan, C. A. Regal, D. L. Feder, L. A. Collins, C. W. Clark, and E. A. Cornell, Watching Dark Solitons Decay Into Vortex Rings in a Bose-Einstein Condensate, Phys. Rev. Lett. **86**, 2926 (2001).

[11] S.-P. Gorza, B. Deconinck, Ph. Emplit, T. Trogdon, and M. Haelterman, Experimental Demonstration of the Oscillatory Snake Instability of the Bright Soliton of the $(2+1)$**D** Hyperbolic Nonlinear Schrödinger Equation, Phys. Rev. Lett. **106**, 094101 (2011).

[12] S.-P. Gorza, B. Deconinck, T. Trogdon, P. Emplit, and M. Haelterman, Neck instability of bright solitons in normally dispersive Kerr media, Opt. Lett. **37**, 4657 (2012).

[13] Z. H. Musslimani, M. Segev, A. Nepomnyashchy, and Yu. S. Kivshar, Suppression of transverse instabilities for vector solitons, Phys. Rev. E **60**, R1170 (1999).

[14] Z. H. Musslimani and J. Yang, Transverse instability of strongly coupled dark-bright Manakov vector solitons, Opt. Lett. **26**, 1981 (2001).

[15] C. Anastassiou, M. Soljacic, M. Segev, E. D. Eugenieva, D. N. Christodoulides, D. Kip, Z. H. Musslimani, and J. P. Torres, Eliminating the Transverse Instabilities of Kerr Solitons, Phys. Rev. Lett. **85**, 4888 (2000).

[16] J. Yang, Transversely stable soliton trains in photonic lattice, Phys. Rev. A **84**, 033840 (2011).

[17] J. Yang, D. Gallardo, A. Miller, and Z. Chen, Elimination of transverse instability in stripe solitons by one-dimensional lattices, Opt. Lett. **37**, 1571 (2012).

[18] M. Ma, R. Carretero-González, P. G. Kevrekidis, D. J. Frantzeskakis, and B. A. Malomed, Controlling the transverse instability of dark solitons and nucleation of vortices by a potential barrier, Phys. Rev. A **82**, 023621 (2010).

[19] A. G. Litvak, V. A. Mironov, G. M. Fraiman, and A. D. Yunakovskii, Thermal self-effect of wave beams in a plasma with a nonlocal nonlinearity, Sov. J. Plasma Phys. **1**, 60 (1975).

[20] D. Suter and T. Blasberg, Stabilization of transverse solitary waves by a nonlocal response of the nonlinear medium, Phys. Rev. A **48**, 4583 (1993).

[21] C. Rotschild, T. Carmon, O. Cohen, O. Manela, and M. Segev, Solitons in Nonlinear Media with an Infinite Range of Nonlocality: First Observation of Coherent Elliptic Solitons and of Vortex-Ring Solitons, Phys. Rev. Lett. **95**, 213904 (2005).

[22] C. Conti, M. Peccianti, and G. Assanto, Route to Nonlocality and Observation of Accessible Solitons, Phys. Rev. Lett. **91**, 073901 (2003).

[23] P. Pedri and L. Santos, Two-Dimensional Bright Solitons in Dipolar Bose-Einstein Condensates, Phys. Rev. Lett. **95**, 200404 (2005).

[24] YuanYao Lin, R.-K. Lee, and Yu. S. Kivshar, Suppression of soliton transverse instabilities in nonlocal nonlinear media, J. Opt. Soc. Am. B **25**, 576 (2008).

[25] S. K. Turitsyn, Spatial dispersion of nonlinearity and stability of many dimensional solitons, Theor. Math. Phys. **64**, 797 (1985).

[26] O. Bang, W. Krolikowski, J. Wyller, and J. J. Rasmussen, Collapse arrest and soliton stabilization in nonlocal nonlinear media, Phys. Rev. E **66**, 046619 (2002).

[27] W. Krolikowski, O. Bang, N. I. Nikolov, D. Neshev, J. Wyller, J. J. Rasmussen, and D. Edmundson, Modulational instability, solitons, and beam propagation in spatially nonlocal nonlinear media, J. Opt. B **6**, S288 (2004).

[28] D. Mihalache, D. Mazilu, F. Lederer, B. A. Malomed, Y. V. Kartashov, L.-C. Crasovan, and L. Torner, Three-dimensional spatiotemporal optical solitons in nonlocal nonlinear media, Phys. Rev. E **73**, 025601(R) (2006).

[29] D. Mihalache, Multidimensional solitons and vortices in nonlocal nonlinear optical media, Rom. Rep. Phys. **59**, 515 (2007).
[30] A. Dreischuh, D. N. Neshev, D. E. Petersen, O. Bang, and W. Krolikowski, Observation of Attraction Between Dark Solitons, Phys. Rev. Lett. **96**, 043901 (2006).
[31] Y. V. Kartashov and L. Torner, Gray spatial solitons in nonlocal nonlinear media, Opt. Lett. **32**, 946 (2007).
[32] A. Piccardi, A. Alberucci, N. Tabiryan, and G. Assanto, Dark nematicons, Opt. Lett. **36**, 1356 (2011).
[33] T. P. Horikis, Small-amplitude defocusing nematicons, J. Phys. A: Math. Theor. **48**, 02FT01 (2015).
[34] A. Armaroli and S. Trillo, Suppression of transverse instabilities of dark solitons and their dispersive shock waves, Phys. Rev. A **80**, 053803 (2009).
[35] N. Ghofraniha, C. Conti, G. Ruocco, and S. Trillo, Shocks in Nonlocal Media, Phys. Rev. Lett. **99**, 043903 (2007).
[36] C. Conti, A. Fratalocchi, M. Peccianti, G. Ruocco, and S. Trillo, Observation of a Gradient Catastrophe Generating Solitons, Phys. Rev. Lett. **102**, 083902 (2009).
[37] A. I. Yakimenko, Y. A. Zaliznyak, and Yu. S. Kivshar, Stable vortex solitons in nonlocal self-focusing nonlinear media, Phys. Rev. E **71**, 065603(R) (2005).
[38] M. Peccianti and G. Assanto, Nematicons, Phys. Rep. **516**, 147 (2012).
[39] A. Alberucci and G. Assanto, Modeling nematicon propagation, Mol. Cryst. Liq. Cryst. **572**, 2 (2013).
[40] M. Z. Pesenson, Nonlinear waves traveling upon a front of solitons, Phys. Fluids A **3**, 3001 (1991).
[41] M. J. Ablowitz and H. Segur, *Solitons and the Inverse Scattering Transform* (SIAM, Philadelphia, PA, 1981).
[42] G. Assanto, *Nematicons: Spatial Optical Solitons in Nematic Liquid Crystals* (Wiley-Blackwell, New Jersey, 2012).
[43] I. A. Kol'chugina, V. A. Mironov, and A. M. Sergeev, Structure of steady-state solitons in systems with a nonlocal nonlinearity, JETP Lett. **31**, 304 (1980).
[44] J. M. L. MacNeil, N. F. Smyth, and G. Assanto, Exact and approximate solutions for solitary waves in nematic liquid crystals, Physica D **284**, 1 (2014).
[45] W. L. Kath and N. F. Smyth, Soliton evolution and radiation loss for the nonlinear Schrödinger equation, Phys. Rev. E **51**, 1484 (1995).
[46] M. J. Ablowitz, S. D. Nixon, T. P. Horikis, and D. J. Frantzeskakis, Perturbations of dark solitons, Proc. R. Soc. A **467**, 2597 (2011).
[47] A. Kassam and L. N. Trefethen, Fourth-order time stepping for stiff PDEs, SIAM J. Sci. Comput. **26**, 1214 (2005).
[48] S. Skupin, O. Bang, D. Edmundson, and W. Krolikowski, Stability of two-dimensional spatial solitons in nonlocal nonlinear media, Phys. Rev. E **73**, 066603 (2006).
[49] P. A. E. M. Janssen and J. J. Rasmussen, Nonlinear evolution of the transverse instability of plane-envelope solitons, Phys. Fluids **26**, 1279 (1983).
[50] Yu. A. Zaliznyak and A. I. Yakimenko, Three-dimensional solitons and vortices in dipolar Bose-Einstein condensates, Phys. Lett. A **372**, 2862 (2008).
[51] V. M. Lashkin, A. I. Yakimenko, and Yu. A. Zaliznyak, Stable three-dimensional vortex solitons in Bose-Einstein condensates with nonlocal dipole-dipole interaction, Phys. Scr. **79**, 035305 (2009).
[52] T. P. Horikis and D. J. Frantzeskakis, Asymptotic reductions and solitons of nonlocal nonlinear Schrödinger equations, J. Phys. A: Math. Theor. **49**, 205202 (2016).
[53] T. P. Horikis and D. J. Frantzeskakis, Ring dark and antidark solitons in nonlocal media, Opt. Lett. **41**, 583 (2016).
[54] T. P. Horikis and D. J. Frantzeskakis, Light Meets Water in Nonlocal Media: Surface Tension in Optics, Phys. Rev. Lett. **118**, 243903 (2017).
[55] A. Alberucci, M. Peccianti, G. Assanto, A. Dyadyusha, and M. Kaczmarek, Two-Color Vector Solitons in Nonlocal Media, Phys. Rev. Lett. **97**, 153903 (2006).
[56] Y. Lin and R.-K. Lee, Dark-bright soliton pairs in nonlocal nonlinear media, Opt. Express **15**, 8781 (2007).
[57] T. P. Horikis and D. J. Frantzeskakis, Vector nematicons: Coupled spatial solitons in nematic liquid crystals, Phys. Rev. A **94**, 053805 (2016).
[58] G. N. Koutsokostas, T. P. Horikis, D. J. Frantzeskakis, B. Prinari, and G. Biondini, Multiscale expansions and vector solitons of a two-dimensional nonlocal nonlinear Schrödinger system, Stud. Appl. Math. **145**, 739 (2020).
[59] G. N. Koutsokostas, T. P. Horikis, D. J. Frantzeskakis, B. Prinari, and G. Biondini, Transverse dynamics of vector solitons in defocusing nonlocal media, Eur. Phys. J. Plus **135**, 546 (2020).